Analysing fluid-structure interaction with CFD and FEA on a marine double-wall LNG piping system

Alihan Cambaz[1], Yasin Furkan Gorgulu[2], Halit Arat[3]

[1] SU Ar-Ge Dizayn ve Mühendislik A.Ş., 77000, Yalova-Turkey, e-mail: cambazalihan7@gmail.com
[2] Department of Machinery and Metal Technologies, Isparta University of Applied Sciences Keciborlu Vocational School, 32750, Isparta-Turkey, e-mail: yasingorgulu@isparta.edu.tr
[3] Mechanical Engineering Department, Kutahya Dumlupinar University Engineering Faculty, 43270, Kutahya-Turkey, e-mail: halit.arat@dpu.edu.tr

ABSTRACT

In this study, the interaction of fluid-structure with Ansys Fluent and Structural was analysed on a double-wall LNG piping system in a marine ship. In terms of simulations, the inner tube of the double-walled tube on the TSR-18008 ship designed by SU Ar-Ge Dizayn ve Mühendislik A.Ş. is considered. Two different simulations were made; the first analysis was a computational fluid dynamics analysis and the results obtained from this were imported into the finite element analysis also known as structural analysis and the structural analysis was undertaken together using these data. The mesh used in the simulations has 2,985,116 elements and 2,135,093 nodes. The inlet velocity of the gas is 6.5 m/s and the temperature value is 108 K as boundary conditions. Seventeen cylindrical support elements are used to ensure the strength of the Liquefied Natural Gas pipe system. Three different pipe materials, which are structural steel, stainless steel, and aluminium alloy, have been considered for the numerical structural analysis. The highest stresses were observed at the elbows and results were given using various contours including stresses, strains, temperatures and streamlines in these elbows.

ARTICLE INFO

1 Introduction

Natural gas being a clean fossil fuel is a significant energy source for human beings [1]. Due to ongoing industrialisation and urbanisation in emerging nations, natural gas is acquiring more and more shares in the global energy system as cleaner energy than other fossil fuels. Liquefied Natural Gas (LNG) is non-corrosive, non-toxic, odourless and colourless. If LNG which is kept in double-wall, well-insulated tanks is mixed with 5–15 percent of air, it will start burning [2]. The entire process, from the exploration, discovery, and production of raw material sources, to regasification of the liquid and delivery to the pipeline, is known as the LNG value chain. [3], [4]. There are four steps of the process; first, the discovery and production of the natural gas; second the liquefaction step, third is the transportation; and lastly, its storage and regasification [5].

Failure of a pipeline can have major results, and there are several risk factors impacting the pipeline's safety [6]. Limit state functions, which define the distinction between failure and safe conditions given to a load and a resistance to fail, are commonly used to assess structural reliability. Resulting in high operation loads, the pressure and temperature impacts, as well as these requirements, are important to address [7]. Due to the risk of a rupture or leak, internal pressure is one of the most important loads evaluated [8]. Moreover, there are some studies about modelling these damages that affected the natural gas pipe strength [9], [10].The structural analysis of the pipeline system is performed in different fields of usage by using numerical models which are composed of various programs. Mladenović et al. [11] have numerically assessed the stress analysis of the welded connection in a steam pipeline by utilizing the finite element approach (Abaqus software) to calculate the stress distribution. On the other hand, Dizdar et al. [12] have numerically investigated the stress analysis of nuclear pipe support by using Pipestress (modelling of the piping system) and Ansys (modelling of pipe support). Moreover, Gu et al. [13] have numerically examined the inner and outer pipes of composite pipes and lined pipe stress analysis, and

also the equivalent pipe parameters are taken into account by using CAESAR II software.

Pipelines have traditionally been the primary mode of transport for natural gas. Transporting liquefied natural gas has steadily gained popularity as a result of technological advancements, supply diversification, and political reasons [14], [15]. Recently, the demand for Liquefied Natural Gas (LNG) used for power generation has been increasing rapidly for these reasons [16].

In this study, a simulation was carried out on the structural analysis of the inner pipe of the double-wall LNG transport line by using the interaction of fluid-structure with Ansys Fluent and Structural.

2 Materials and Methods

2.1 Materials

The global shipping sector is facing some problems because of the International Maritime Organization's (IMO) limitations on ship emissions, which went into effect in 2015 in Emission Control Areas and 2020 for the rest of the globe. As a result of this regulation, sulphur emissions from ships will be considerably reduced. LNG is a potential option for achieving these criteria because it contains almost little sulphur and creates low NOx when burned compared to fuel oil and marine diesel oil [17]. The shipping industry is facing some difficulties when filling LNG tanks. One of the most important difficulties is the pipeline wherefrom the bunker station to the LNG tank during filling. The design

flow is based on an LNG bunkering feed supply with a liquid temperature of -162 C during the bunkering operation, with no gas feed out from the tank connection space [18]. In most cases, double-wall pipes are utilized in the liquid-filled piping system [19]–[21] and pipe elbows [22], [23]. The core pipe is at cryogenic temperature and the Jacket is vacuum normally at ambient temperature while the cryogenic temperature is generally -265 F (-165 °C) or lower [24]. This article presents the 3D finite element method in core pipe of three different pipe material stress analyses with Ansys. While working with cryogenic systems, there are several challenges in cryogenics pipe stress analysis. The most challenging aspect of structural analysis is optimization; the placements of the supports must be chosen while thermal effects are taken into account. More strength does not imply more support. Thermal expansion occurs as a result of thermal processes, and the supports should not be used to prevent this. [24]. Ansys software has been used in fluent and static structure finite element analysis [25]. Bunkering of LNG takes place in a bunkering station. In this study, the bunker line on the ship TSR-18008 is addressed. The primary core bunkering line has a diameter of DN100 and a maximum flow of 220 m³/h [26]. Three different pipe materials on bunker lines were subjected to stress analysis and the flow properties of liquefied natural gas have been studied using Ansys Fluent. The purpose of this research is to estimate the stress using the Computational Fluid Dynamics (CFD) technique because momentum will be generated in the pipeline under the influence of flow. As a result, it offers substantial advantages in terms of identifying locations of severe stress, reduced uncertainty, and a com-
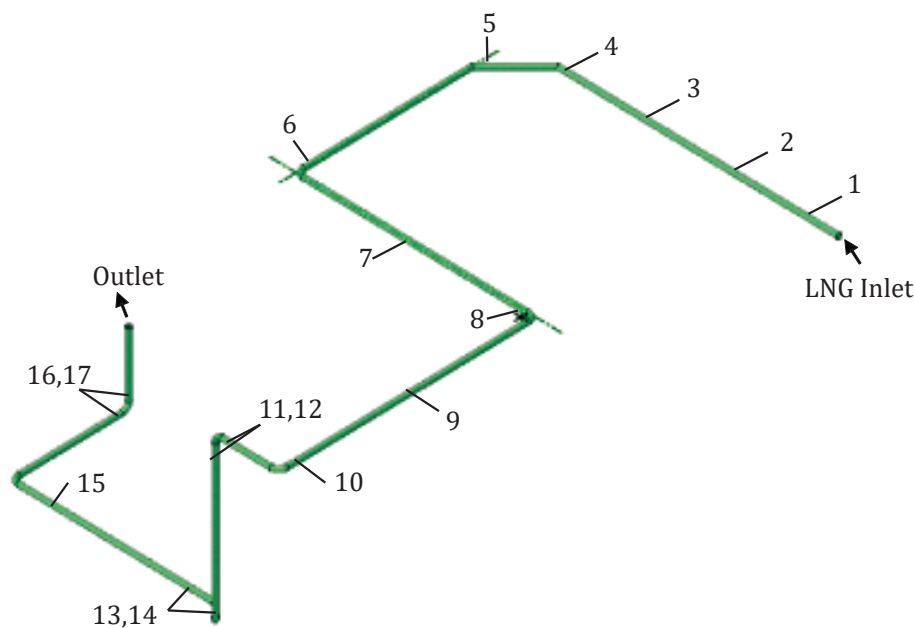
Figure 1 The bunker station line design

Table 1 The structural properties of discussed three pipe materials

Pipe Material	Strength (Pa)	Young Modulus (Pa)	Poisson's Ratio	Shear Modulus (Pa)
Structural Steel	2.40×10^8	2.00×10^{11}	0.30	7.60×10^{10}
Stainless Steel	2.05×10^8	1.93×10^{11}	0.31	7.30×10^{10}
Aluminium Alloy	2.70×10^8	7.10×10^{10}	0.33	2.66×10^{10}

Source: Authors

prehensive set of modelling skills for complicated flows. A bunkering line of 20 m pipe, ten bends with a flow speed of 6.5 m/s is the design flow under consideration. The bunker station line design is shown in Figure 1 as well as the liquid natural gas inlet and the outlet.

2.2 Methods

Ansys Fluent and Static Structure has been used as the stress simulation program in the study. The flow characteristic was studied using the Fluent analysis tool, while the pipe stress was studied using Static Structure analysis. To better understand the liquid natural gas flow, Realizable k-epsilon (k-ε) turbulence with enhanced wall treatment with thermal effect and pressure gradient effects model has been used in the simulations. Realizable k-ε shows a greater performance to capture the mean flow of complicated structures in nearly every comparison. It also performs other flow types better, such as boundary layers under high-pressure gradients, recirculation rotation, and separation [27]–[29]. Ansys placed control mechanisms such as orthogonal quality and skewness ratios for understanding the quality of the mesh. It is recommended the average skewness values be between the range of 0.25-0.50 is a very good quality mesh. For the orthogonal quality, that range reaches out to values of 0.20-0.69, and it is considered good quality [30], [31]. In our case, the average mesh skewness is 0.42, and the average orthogonal quality of the mesh is 0.62. The mesh used in the simulation has 2,985,116 elements and 2,135,093 nodes. Gas enters the tube with a velocity of 6.5 m/s and a temperature value of 108 K. After the fluent analysis has been finished, the values of analysis have been used to imported into the static structure analysis. Three different pipe materials which are structural steel, stainless steel and aluminium alloy have taken into account for the numerical structural analysis. The structural properties of these three materials are given in Table 1.

Due to the LNG's low temperature, the pipeline expands or shrinks. When a pipe expands, the entire pipeline extends to make room for its movement. If the piping system does not have enough flexibility to absorb this expansion, the force and stress generated can be large enough to damage the piping and the connecting equipment [32]. Figure 1 shows a bunker pipe connected to 17 cylindrical supports. Cylindrical support constrains the pipe movement radially and tangentially. The cylindrical supports implemented in structural steel analysis are the ideal support for the pipe system. In this study, when the temperature of a straight pipe changes due to transporting LNG, it causes the pipe to expand. The supports on the pipe, on the other hand, prevent the pipe from expanding [32]. Stress analysis and displacements have been observed on three different materials with the thermal effect from the fluent. Rather than specifying a static temperature, the temperature and momentum produced by the flow's movement are used.

2.2.1 Stress Analysis Method

The conventional technique of determining a material's strength is to stretch the specimen to failure and measure its tensile strength. The American Society for Testing and Materials (ASTM) [33] has established a standard for testing and interpretation of findings since test results vary greatly depending on specimens and processes. The test not only determines the material's ultimate strength but also establishes the link between the applied force and the specimen's elongation by progressively increasing the force [32]. Stress (*S*) being the amount of force per unit cross-section area and strain (*e*) called the amount of elongation per unit length of the specimen are calculated at each stage of the testing by using the following equations:

$$S = \frac{F}{A} \tag{1}$$

$$e = \frac{l}{L} \tag{2}$$

Where:

    F = applied force
    A = cross-section area of the specimen
    L = length of the specimen
    l = elongation of the specimen

The connections between applied force in terms of stress and the elongation generated are shown in Figure 2. The stress/strain ratio is constant in the elastic range. Hooke's Law is the name given to this connection. The modulus of elasticity (*E*), often known as Young's modulus, is the proportional constant. Equation 3 can be derived from the equations 1 and 2, which are shown below:

$$E = \frac{S}{e} \tag{3}$$

Where:

    E = Modulus of Elasticity
    S = Stress
    e = Strain

(a), Curve with Yield Point   (b), Round House Curve
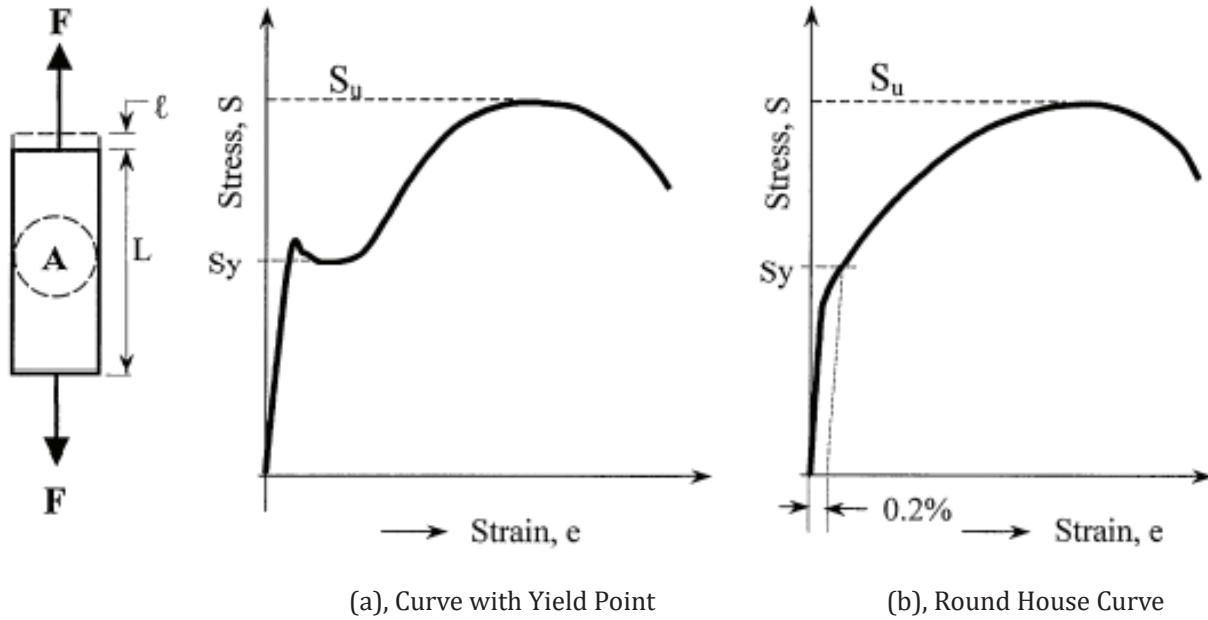
Figure 2 Stress and strain relations [32]

2.2.2 Effective Stress (Von-Mises Stress)

The maximum distortion energy failure theory is the most compatible with the properties of ductile materials and this idea is highly popular in the European Piping Community. Von-Mises stress diagram expressed by six stress components is shown in Figure 3 and the prerequisite for yielding, according to distortion energy theory is [34]:
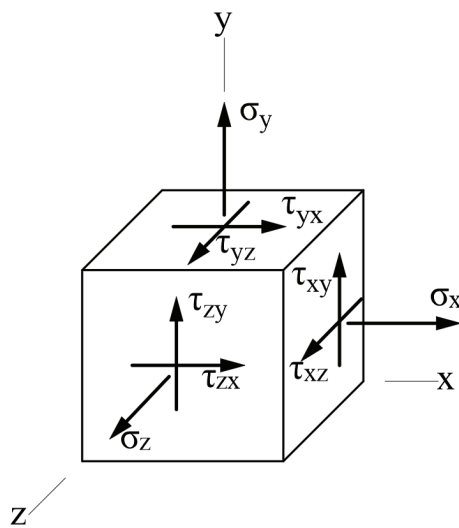
Figure 3 Von-Mises stress diagram expressed by six stress components [35]

$$\sigma_{vm} = \sqrt{0.5[(\sigma_x - \sigma_y)^2 + (\sigma_y - \sigma_z)^2 + (\sigma_z - \sigma_x)^2] + 3(\tau_{xy}{}^2 + \tau_{yz}{}^2 + \tau_{zx}{}^2)} \quad (4)$$

When the stress on the structure is examined in three dimensions, it is seen that σ_x, σ_y and σ_z normal stresses exist perpendicular to each of the structure's surfaces. Each 2-dimensional portion of the structure experiences axial and radial shear loads. These shear stresses have components that are parallel to the surface components. These components are τ_{xy}, τ_{yz} and τ_{zx}, respectively.

3 Results and Discussion

When the whole LNG pipe system is considered, it is seen that maximum stresses and deformations occur mainly in the five elbows. The locations of the elbows and the spots where the maximum and minimum stresses occur are shown in Figure 4.

In Figure 5, stress-strain contours of structural steel, stainless steel and aluminium alloy are illustrated. The maximum Von-Mises stress of 40.197 MPa is observed in the aluminium alloy at the Elbow 1, while the minimum stress is seen as 1.1729 MPa. For the stainless steel, the maximum Von-Mises stress is measured as 78.628 MPa and the minimum is 2.1125 MPa. Structural steel stands in the middle of other materials in terms of stress values. Materials follow a similar trend for the strain values. The aluminium alloy has a maximum value of 0.1352 mm which is the highest value among other materials.

70.698 MPa is the highest maximum Von-Mises value measured from the Elbow 2 in stainless steel material. The aluminium alloy shows the minimum Von-Mises stress with 1.3038 MPa. The greatest strain reaches a value of 0.12949 mm in the aluminium alloy. Structural steel has the least strain with 0.014841 mm. Stress-strain contours of Elbow 2 are shown in Figure 6.
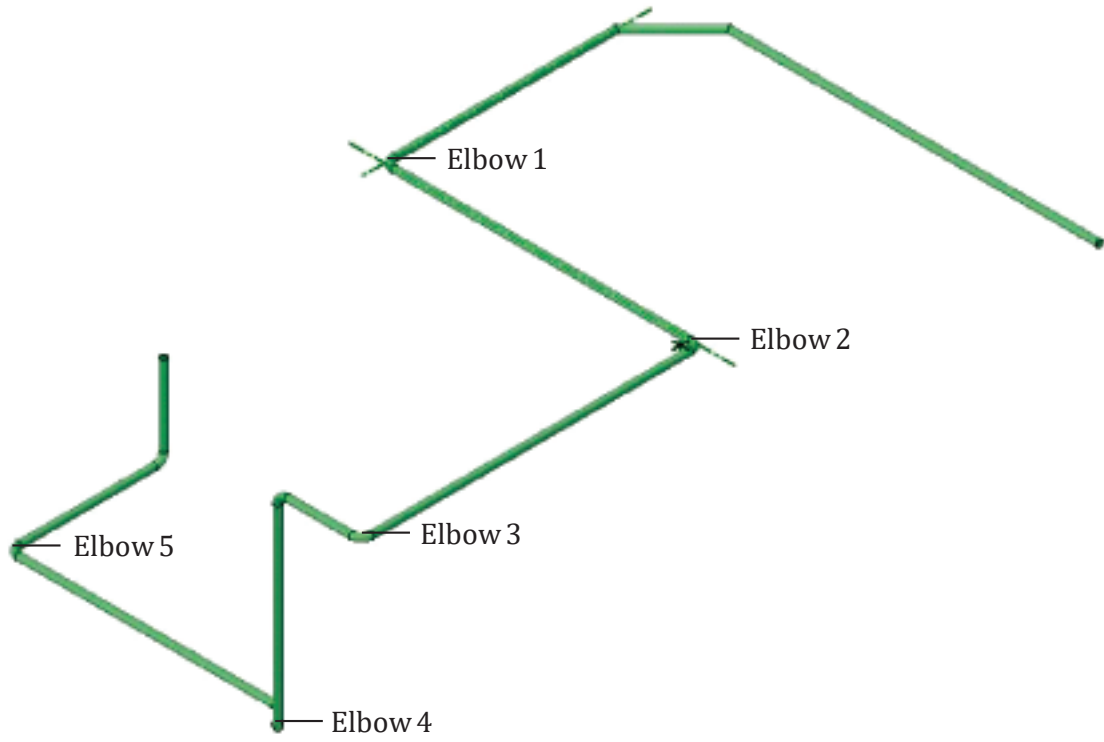
Figure 4 The layout of the analysed elbows

Source: Authors
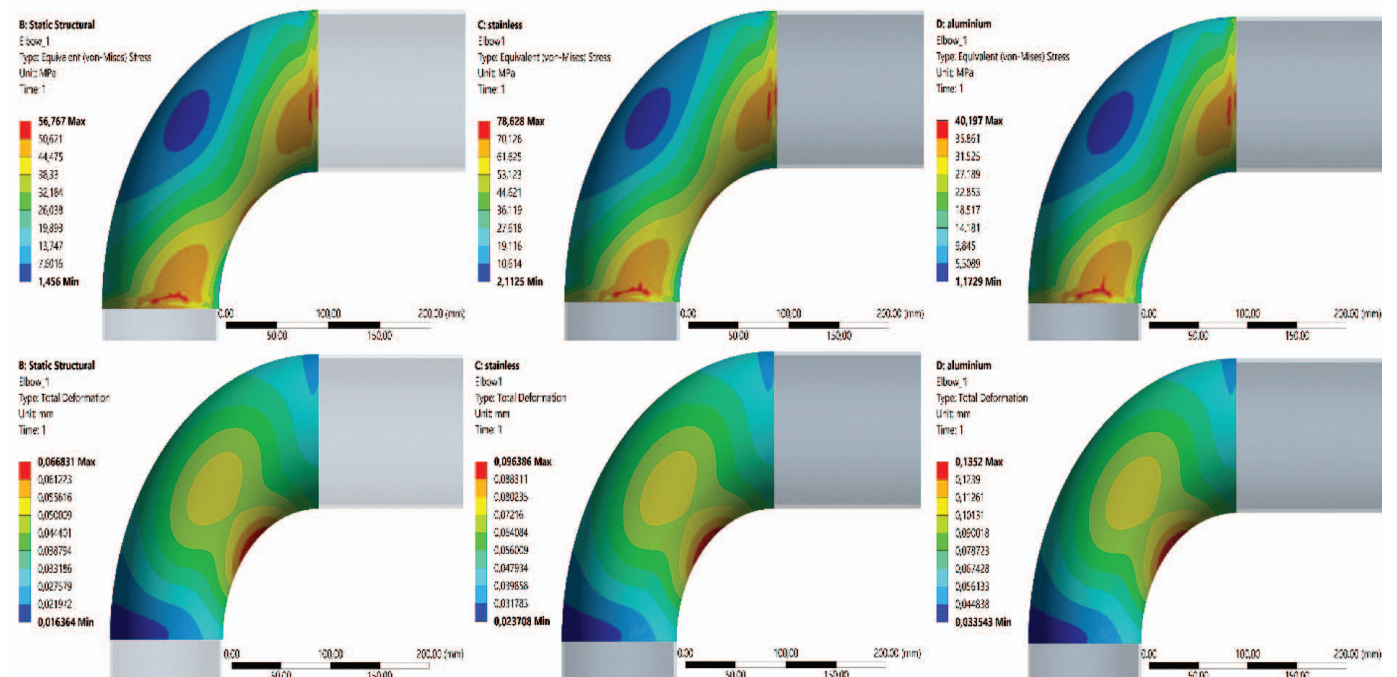
Figure 5 Stress and strain contours on Elbow 1 for the three pipe materials
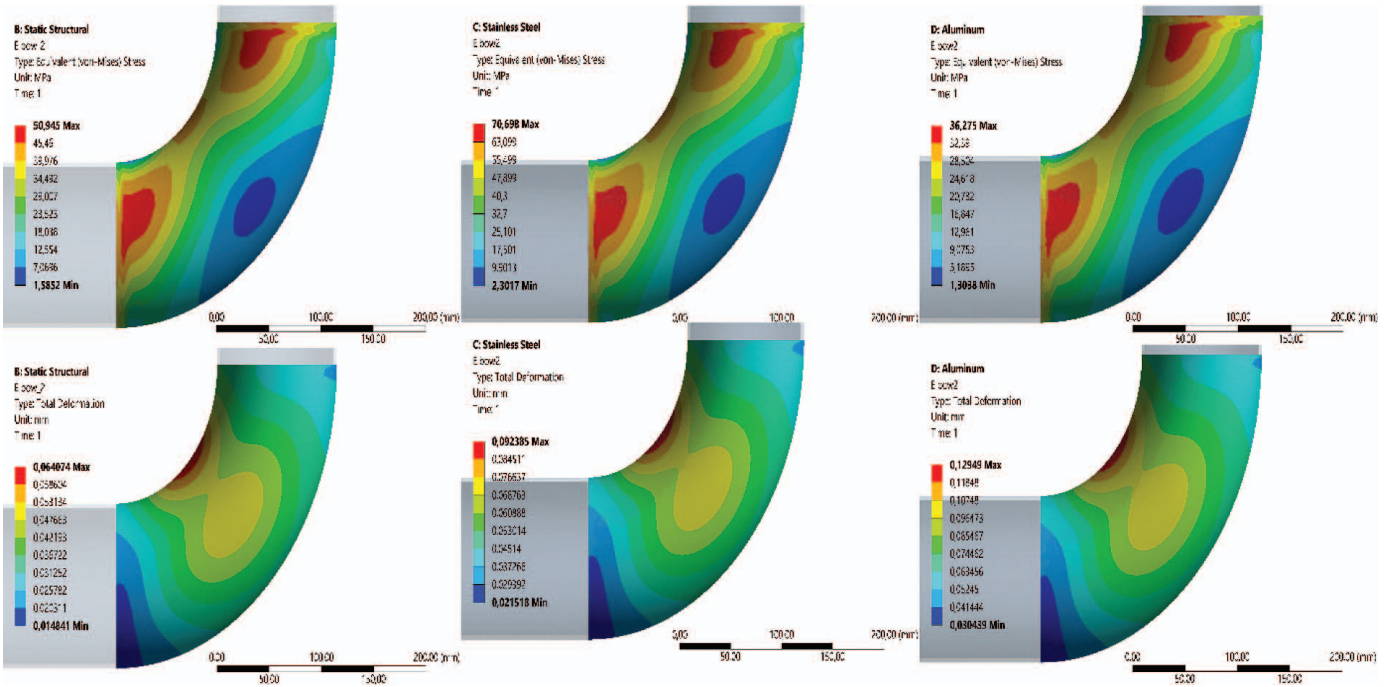
Source: Authors

Figure 6 Stress and strain contours on Elbow 2 for the three pipe materials

Source: Authors

As seen in the first two elbows, similarly, the maximum stress in the Elbow 3 occurs with a Von-Mises stress value of 76.624 MPa in the stainless steel. Minimum Von-Mises stress is seen in the aluminium alloy with a 1.1355 MPa value. The stress-strain contours of the Elbow 3 are dem-onstrated in Figure 7. The greatest deformation occurs in the aluminium alloy and its value is 0.12289 mm, whilst the smallest value which is 0.0019767 mm belongs to the structural steel.
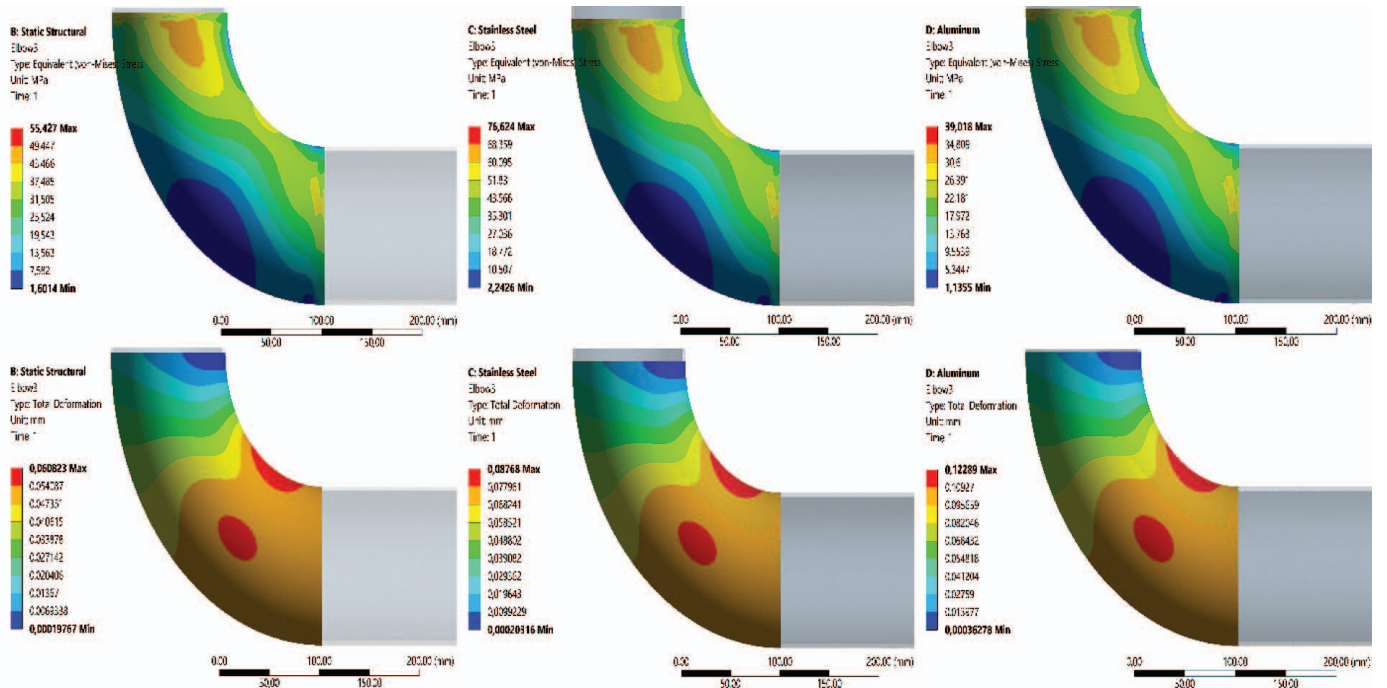
Figure 7 Stress and strain contours on Elbow 3 for the three pipe materials

Source: Authors

The maximum and the minimum values of stress/ strain in the whole system occur in the Elbow and the contours are illustrated in Figure 8. The maximum Von-Mises stress occurs in the stainless steel with 103.3 MPa while the lowest with 0.3703 MPa in the aluminium alloy. Likewise, strain values perform similarly. The maximum deformation is 0.33962 mm in the aluminium alloy. The minimum deformation is 0.019151 mm in the structural steel. It is observed that the dramatic turns are the greatest source of the Von-Mises stresses. There is a need for improvement in the Elbow 4.
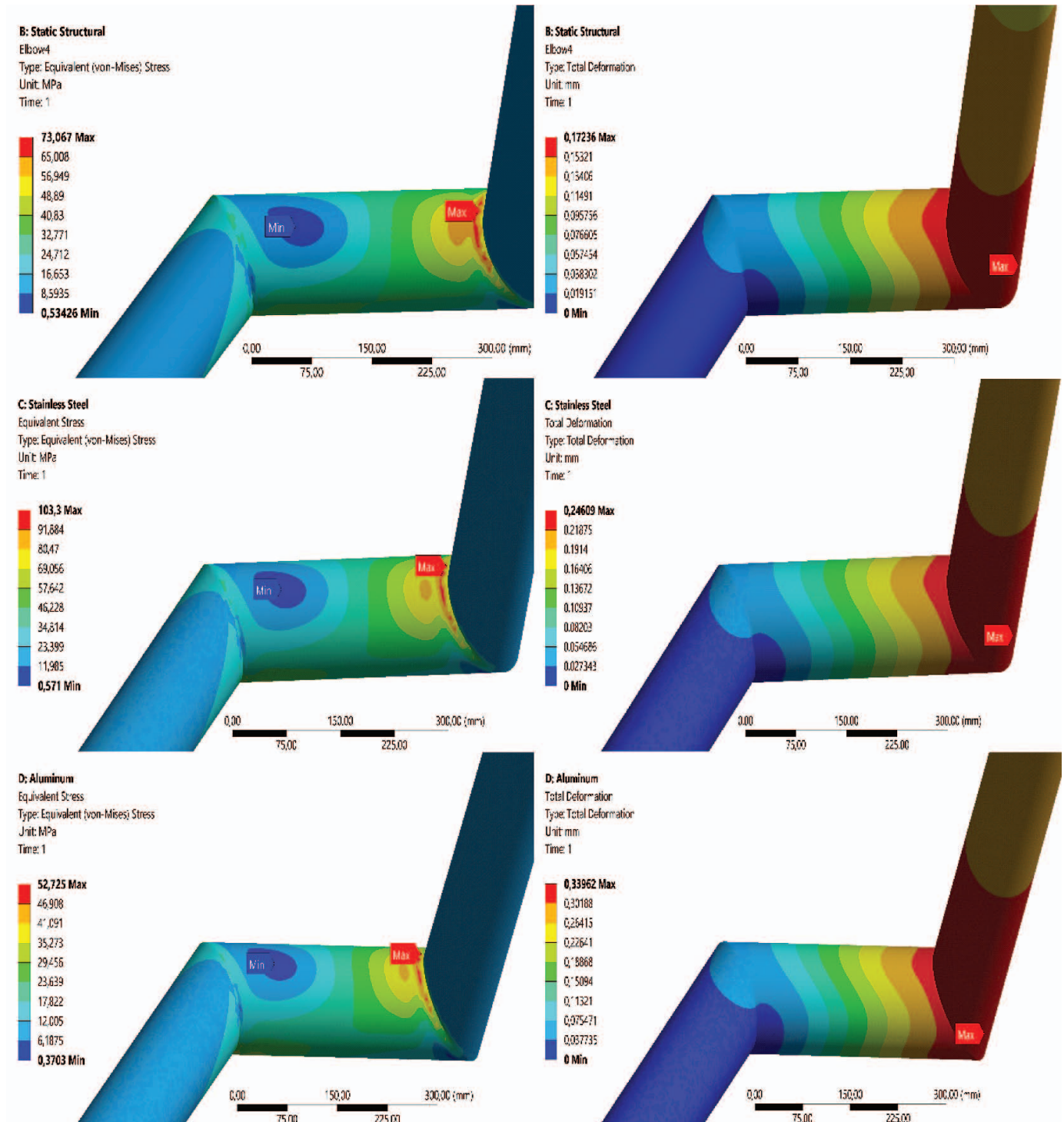
Figure 8 Maximum and minimum stress and strain spots on the piping system (Elbow 4) for the three pipe materials

Source: Authors

The Elbow 5 also exhibits similar stress-strain performance to the other first four elbows. The maximum Von-Mises stress of 73.227 MPa is observed in the stainless steel at the Elbow 5, while the minimum stress is seen as 1.2368 MPa in the aluminium alloy. In the case of strains, the maximum total deformation is seen in the aluminium alloy with 0.12657. On the other hand, the minimum deformation is performed by the structural steel with a value of 0.0072618 mm. Elbow 5's stress-strain contours are given in Figure 9.
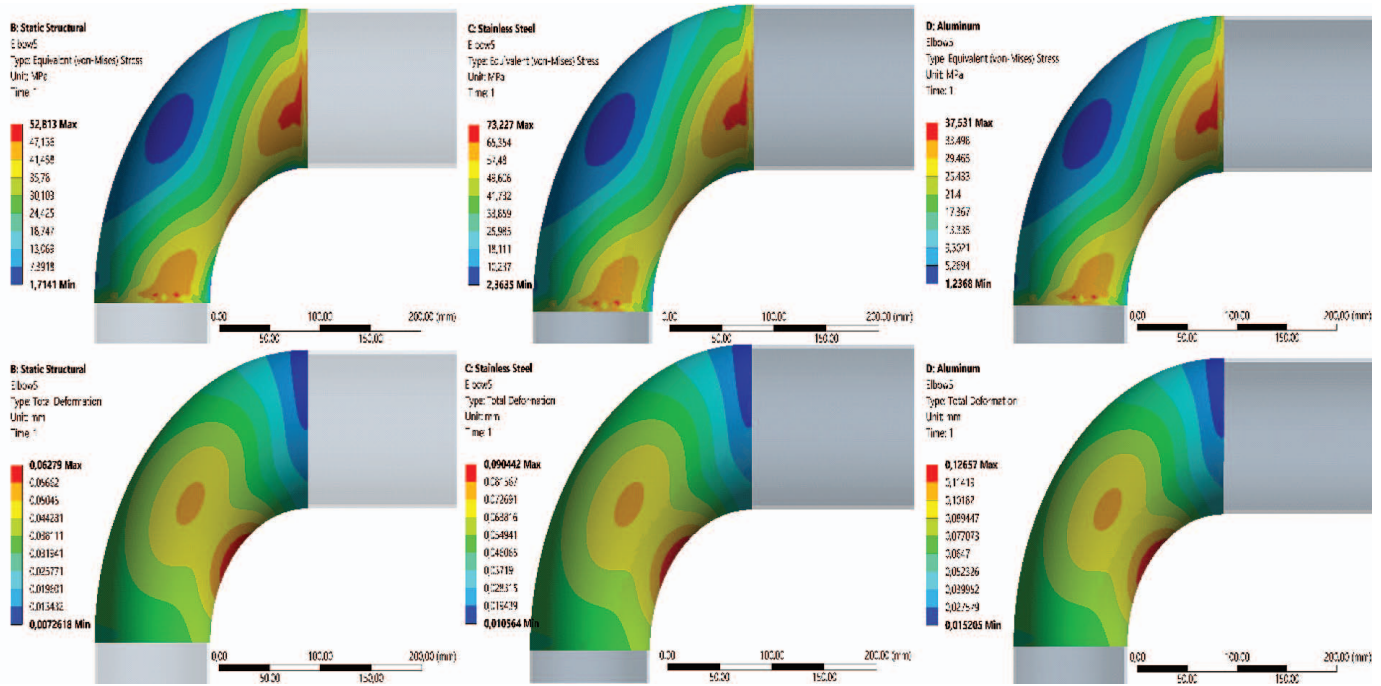
Figure 9 Stress and strain contours on Elbow 5 for the three pipe materials
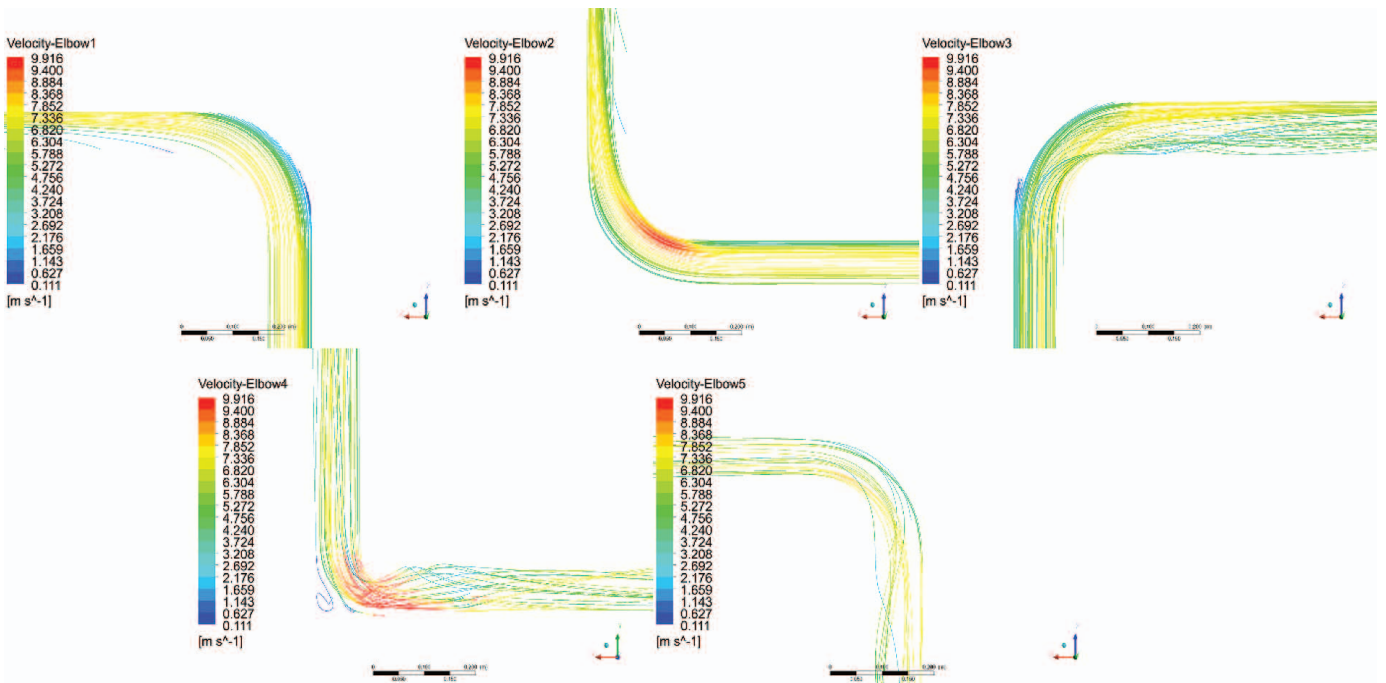
Source: Authors

Figure 10 Velocity streamlines views of the elbows

Source: Authors

Velocity streamlines are demonstrated for the five elbows simulated in Figure 10. 90-degree turns cause slowdowns or even stops in the flows in the elbows. Using elbows with lower angles can allow for smoother flow transitions.

4 Conclusions

The interaction of fluid-structure with Ansys Fluent and Structural was analysed on the inner pipe of the double-wall LNG piping system in the TSR-18008 ship. Two different simulations were made; the first analysis was a CFD, and the results obtained from this were imported into the FEA also known as structural analysis and the structural analysis was undertaken together using these data.

According to simulation results, the highest Von-Mises stress occurs at Elbow 4 with a value of 103.3 MPa in the stainless steel. The lowest stress value is also seen at Elbow 4 with 0.3703 MPa in the aluminium alloy. The maximum deformation is 0.33962 mm in the aluminium alloy.

Stress-strain contours show where they hit the maximum and the minimum. Especially, the elbows with dramatic angles should need improvements to ease the stress and strain. When an elbow is exposed to thermal stressors, the long radius variant expands more than the short radius version. By producing centrifugal force, increasing the radius of curvature can produce secondary flows perpendicular to the flow direction. The cryogenic fluid cannot hang on to the boundary layer because its viscosity is too low. Because the system's maximum backpressure value is the most important aspect in these circumstances, the total backpressure value as well as the places where secondary flows occur should be optimized. The fluid movement may be maintained by forming systems from elbows with long and short radii. Long bending radiuses will push the system more, and the supports on the elbows will prevent expansion and cause higher tension in cryogenic systems.

Author Contributions: Each author evaluated the data and proposed an analytical method. The writers collaborated to conduct a case study using finite element analysis. Each author contributed equally to the project.

References

[1] International Energy Agency IEA, "World Energy Outlook 2019," 2019 [Online]. Available: https://webstore.iea.org/download/summary/2467?fileName=Japanese-Summary-WEO2019.pdf.

[2] J. Javanmardi, K. Nasrifar, S. H. Najibi, and M. Moshfeghian, "Feasibility of transporting LNG from South-Pars gas field to potential markets," *Appl. Therm. Eng.*, vol. 26, no. 16, pp. 1812–1819, 2006, doi: 10.1016/j.applthermaleng.2006.02.003.

[3] J. Hu, F. Khan, and L. Zhang, "Dynamic resilience assessment of the Marine LNG offloading system," *Reliab. Eng. Syst. Saf.*, vol. 208, no. April 2020, p. 107368, 2021, doi: 10.1016/j.ress.2020.107368.

[4] R. N. Krikkis, "A thermodynamic and heat transfer model for LNG ageing during ship transportation. Towards an efficient boil-off gas management," *Cryogenics (Guildf).*, vol. 92, pp. 76–83, 2018, doi: 10.1016/j.cryogenics.2018.04.007.

[5] Z. Zhu and D. Maxwell, "Natural Gas Prices, LNG Transport Costs, and the Dynamics of LNG Imports," *Energy Econ.*, 2011, doi: 10.1016/j.eneco.2010.06.012.

[6] Z. J. WANG, Z. H. WEN, J. P. ZHOU, L. GENG, B. F. AN, and W. D. CHEN, "Submarine Transportation Pipeline Safety Assessment System and Its Application," *Corros. Prot.*, vol. 33, no. 10, pp. 903–907, 2012.

[7] L. Muravyeva and N. Vatin, "The safety estimation of the marine pipeline," in *Applied Mechanics and Materials*, 2014, vol. 633–634, doi: 10.4028/www.scientific.net/AMM.633-634.958.

[8] R. Amaya-Gómez, M. Sánchez-Silva, E. Bastidas-Arteaga, F. Schoefs, and F. Muñoz, "Reliability assessments of corroded pipelines based on internal pressure – A review," *Engineering Failure Analysis*, vol. 98. 2019, doi: 10.1016/j.engfailanal.2019.01.064.

[9] Z. Rui, G. Han, H. Zhang, S. Wang, H. Pu, and K. Ling, "A new model to evaluate two leak points in a gas pipeline," *J. Nat. Gas Sci. Eng.*, vol. 46, 2017, doi: 10.1016/j.jngse.2017.08.025.

[10] Y. Zhuohua, Y. Qing, J. Zhenzhen, and L. He, "Numerical Simulation of Pipeline-Pavement Damage Caused by Explosion of Leakage Gas in Buried PE Pipelines," *Adv. Civ. Eng.*, vol. 2020, 2020, doi: 10.1155/2020/4913984.

[11] S. M. Mladenović *et al.*, "Numerical analysis of thermal stresses in welded joint made of steels X20 and X22," *Therm. Sci.*, vol. 18, pp. 121–126, 2014, doi: 10.2298/TSCI131211178M.

[12] S. Dizdar, A. Vucina, N. Rasovic, and R. Tomovic, "Application of pipestress and ansys in stress analysis of nuclear pipe support – Case study," in *IOP Conference Series: Materials Science and Engineering*, 2018, vol. 393, no. 1, doi: 10.1088/1757-899X/393/1/012021.

[13] T. Gu, Q. Zhang, Z. Lian, H. Yu, and J. Chen, "Research and application of equivalent pipe model in stress analysis of lined pipe systems," *Int. J. Press. Vessel. Pip.*, vol. 192, no. April, p. 104418, 2021, doi: 10.1016/j.ijpvp.2021.104418.

[14] M. Schach and R. Madlener, "Impacts of an ice-free Northeast Passage on LNG markets and geopolitics," *Energy Policy*, vol. 122, no. July, pp. 438–448, 2018, doi: 10.1016/j.enpol.2018.07.009.

[15] L. Dai, D. Jing, H. Hu, and Z. Wang, "An environmental and techno-economic analysis of transporting LNG via Arctic route," *Transp. Res. Part A Policy Pract.*, vol. 146, no. December 2019, pp. 56–71, 2021, doi: 10.1016/j.tra.2021.02.005.

[16] M. Watanabe, R. Takada, T. Okafuji, H. Tsujii, M. Kashiwagi, and Y. Kamitani, "Structural Design and Construction Method for 'Apple-Shaped Liquefied Natural Gas Cargo Tank' for LNG Carriers," *Mitsubishi Heavy Ind. Tech. Rev.*, vol. 53, no. 2, pp. 11–18, 2016.

[17] LR-Marine, "LR Marine Bunker Pipe Systems," 2021.

[18] Wartsila, "3 Fuel Storage and Treatment," 2020.

[19] C. S. W. Lavooij and A. S. Tusseling, "Fluid-structure interaction in liquid-filled piping systems," *J. Fluids Struct.*, vol. 5, no. 5, pp. 573–595, 1991, doi: 10.1016/S0889-9746(05)80006-4.

[20] A. S. Tijsseling, "Fluid-structure interaction in liquid-filled pipe systems: A review," *J. Fluids Struct.*, vol. 10, no. 2, pp. 109–146, 1996, doi: 10.1006/jfls.1996.0009.

[21] Y. Gao, F. Sui, J. M. Muggleton, and J. Yang, "Simplified dispersion relationships for fluid-dominated axisymmetric wave motion in buried fluid-filled pipes," *J. Sound Vib.*, vol. 375, pp. 386–402, 2016, doi: 10.1016/j.jsv.2016.04.012.

[22] N. Jaćimović, Z. Ivančić, and M. Ivošević, "Finite element analysis of 90 degree pipe elbow sustained stress indices," *Int. J. Press. Vessel. Pip.*, vol. 192, no. April, 2021, doi: 10.1016/j.ijpvp.2021.104401.

[23] A. S. Tijsseling, A. E. Vardy, and D. Fan, "Fluid-structure interaction and cavitation in a single-elbow pipe system," *J. Fluids Struct.*, vol. 10, no. 4, pp. 395–420, 1996, doi: 10.1006/jfls.1996.0025.

[24] Rishabh Engineering, "Cryogenic Piping Stress Analysis," 2021. https://www.rishabheng.com/blog/cryogenic-pipe-stress-analysis/ (accessed Oct. 02, 2021).

[25] H. Xing, X. Zhang, Z. Liu, and L. Jin, "Piping Stress Analysis of Low Temperature Storage Tank for LNG," *Adv. Mater. Res.*, vol. 512–515, pp. 965–968, 2012, doi: 10.4028/www.scientific.net/AMR.512-515.965.

[26] Wartsila, "Installation Planning Instructions," 2021.

[27] J. E. Bardina, P. G. Huang, and T. J. Coakley, "Turbulence modeling validation," *28th Fluid Dyn. Conf.*, no. April, 1997, doi: 10.2514/6.1997-2121.

[28] "K-epsilon models," 2011. https://www.cfd-online.com/Wiki/K-epsilon_models (accessed Sep. 08, 2021).

[29] T. S. Nesbitt, J. A. Arevalo, J. L. Tanji, W. A. Morgan, and B. Aved, "Will family physicians really return to obstetrics if malpractice insurance premiums decline?," *J. Am. Board Fam. Pract.*, vol. 5, no. 4, pp. 413–418, 1992, doi: 10.3122/jabfm.5.4.413.

[30] Ansys Inc., "Introduction to Ansys Meshing." Ansys Inc., pp. L5–16, 2011.

[31] Y. F. GORGULU, M. A. OZGUR, and R. KOSE, "CFD analysis of a NACA 0009 aerofoil at a low reynolds number," *J. Polytech.*, vol. 0900, pp. 0–1, 2021, doi: 10.2339/politeknik.877391.

[32] L.-C. Peng and T.-L. Peng, *Pipe Stress Engineering*. 2009.

[33] "ASTM International – Standards Worldwide." https://www.astm.org/ (accessed Oct. 04, 2021).

[34] J. H. Wilkinson and C. Reinsch, *Handbook for Automatic Computation: Volume II: Linear Algebra*. Springer-Verlag Berlin Heidelberg, 1971.

[35] R. Patel *et al.*, "A Transdisciplinary Approach for Analyzing Stress Flow Patterns in Biostructures," *Math. Comput. Appl.*, vol. 24, no. 2, p. 47, 2019, doi: 10.3390/mca24020047.